3D dynamic ring-based forwarder selection to improve packet delivery in ultra-dense nanonetworks

Farah Hoteit[a], Eugen Dedu[a], Dominique Dhoutaut[a], Winston K.G. Seah[b]

[a] *Université de Franche-Comté, CNRS, institut FEMTO-ST, firstName.lastName@univ-fcomte.fr, Montbéliard, France*
[b] *School of Engineering and Computer Science, Victoria University of Wellington, winston.seah@ecs.vuw.ac.nz, Wellington, New Zealand*

Abstract

A nanonetwork is a multi-hop network composed of tiny communicating components, whose energy budget is rather limited. A method to reduce the energy used by nodes is to reduce the number of packets transmitted. In this article, we propose a dynamic 3D scheme to reduce the number of forwarders during routing. In this scheme, potential forwarders are found on a ring around transmitter nodes. We analyze the effectiveness of our 3D scheme for four routing protocols in multi-source scenarios. We analyze its memory cost, both theoretically and by simulation. Results show that the proposed scheme works in 3D, and reduces the number of forwarders while maintaining almost the same packet delivery ratio.

Keywords:
Routing, 3D, Nanonetwork, Dense network, Scalability

1. Introduction

The Internet of Things (IoT) creates an inter-connected world of billions of devices ranging from computers to simple sensors, to enable smart services and applications. Although the Covid-19 virus pandemic has had an effect on the adoption of IoT technologies by the time of this article, IoT is continuously growing and the number of connected IoT devices is estimated to be 14.4 billion globally in 2022, according to the State of IoT report [1]. The high demand of applications collecting real-time data about the environment requires a large number of wirelessly connected devices, which need to be low-power and deployed densely in the network. Ultra-dense ad hoc

networks connect these devices and allow them to collaborate in a distributed way, using unicast or multicast communications.

Similarly, driven by the miniaturization race, the Internet of Nano Things (IoNT) connects nanodevices, enabled by nanotechnology, with the internet. Nanotechnology allows the manipulation of materials at the nanoscale. The IoNT may also combine nanonetworks with other networks and technologies, such as Cloud Computing and Big Data [2].

Communication among nanodevices in a nanonetwork can be electromagnetic, molecular, acoustic and mechanical. Most promising communications are molecular and electromagnetic [3]. Molecular nanocommunications are very specific: they use *biological molecules* as data carriers between nanomachines, and have specific transmission characteristics (e.g., very low information transmission speed due to very low molecule velocity, and encoding techniques based on temporal concentration of molecules or on their internal parameters) and applications (e.g., work only in living bodies where molecules exist, and the message is a molecule contrary to traditional communication where the message is text, voice or video) [3]. Electromagnetic nanocommunications rely on the modulation and the demodulation of traditional electromagnetic signals between nanodevices and they are the subject of this article.

1.1. Motivations

In electromagnetic nanonetworks, nodes have a tiny size, hence the energy consumption is critical. Packet transmission is a major source of consumption. Given that communication ranges are small, packets sent by the source are re-transmitted by forwarders (multi-hop routing) in order to reach the destination(s).

We define the large-scale ultra-dense ad hoc networks as networks with more than 10^3 nodes, and with a local node density of at least hundreds of neighbors per node. Such networks are needed for some in-body applications, which require networks of 10^3 to 10^9 nodes with node density exceeding 10^3 nodes per cm^3, and for software-defined metamaterials, where networks usually have 10^3 to 10^9 nodes with a local density of 10^2 to 10^4 nodes per cm^2 [4].

In these networks, selecting the forwarders also becomes critical, as one has to occupy a small number of nodes with the forwarding process, while maintaining a successful packet delivery towards the destination(s), in order to improve the network's performance and to prolong the network's lifetime.

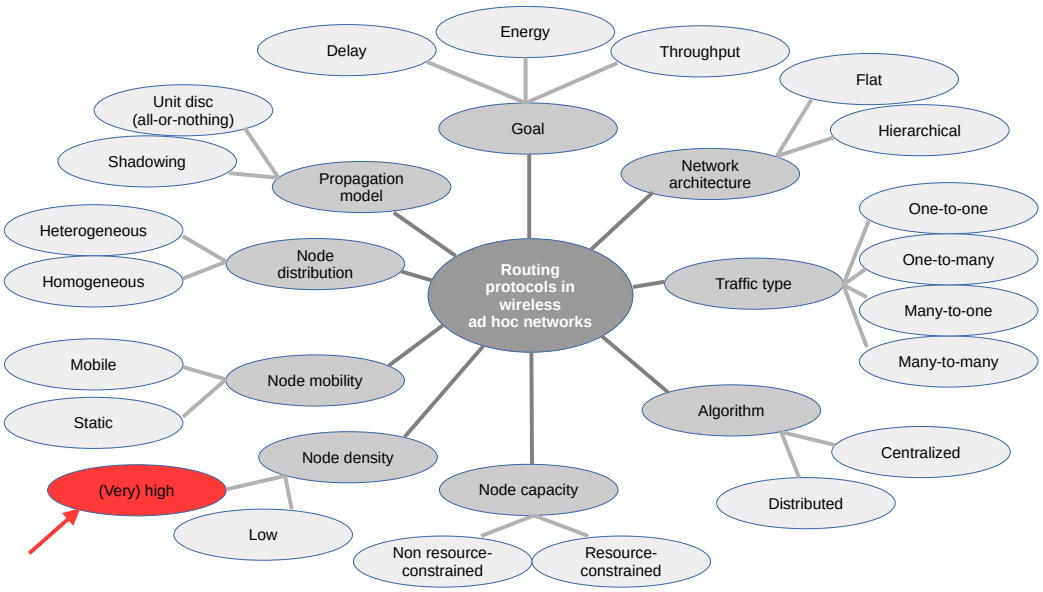

Figure 1: Classification of routing protocols in wireless ad hoc networks.

However, the traditional routing protocols choose a large number of nodes as forwarders, as they do not consider high node densities, as seen in Fig. 1, that is a simplified classification of routing protocols in wireless ad hoc networks. Thus, in large-scale ultra-dense ad hoc networks, most communication protocols become inefficient or are no longer applicable, particularly for resource-constrained nodes that cannot store or process data of neighborhood. Moreover, the additional traffic added by the communication protocols pushes network to congestion, especially in dense environments.

We previously researched three previous works, where we respectively proposed three ring-based forwarder selection schemes to improve packet delivery in ultra-dense networks. The first scheme is the original ring that selects the forwarders on the border of the communication ranges on each transmitting hop [5]. The second scheme is the expanded ring that improves the original ring in multi hop case, where nodes can be on ring for some transmitters, and not on ring for other transmitters [6]. The dynamic ring automatically adapts the original ring's width to the local density [7].

1.2. Contributions

In this article we make the following contributions:

- We extend the dynamic ring scheme to 3D.
- We analyze the scheme in 3D scenarios, in particular its memory cost that implies other resource costs (processing power, speed, energy).
- We simulate multiple sources (and destinations) in the scenario and understand the multi-sources' scenario by validation using four routing protocols: three flooding schemes: pure flooding, probabilistic flooding and backoff flooding, and one destination-oriented scheme: SLR (Stateless Linear-path Routing), applied to an electromagnetic nanonetwork scenario. Although choosing a nanonetwork scenario, the study stays valid for (resource-constrained) ultra-dense ad hoc networks in general. Simulations confirms the dynamic ring is valid in 3D, for multi-source scenario and that the memory cost of the ring is lightweight.

The remaining of the article is organized as follows. Section 2 presents the state of the art. Section 3 presents the system model. Section 4 presents the 3D dynamic ring scheme and its theoretical memory cost. Section 5 presents the results of simulation in various scenarios. Section 6 draws some conclusions.

2. State of the art

2.1. Applications of electromagnetic nanonetworks

Electromagnetic nanonetworks are expected to revolutionize various application domains, as nanomachines can perform tasks of sensing and actuation at an unprecedented small scale [8]. In this section, we list the envisioned application domains of these networks.

One application is to nanomedicine. Nanosensors are comparable in size to some proteins, and they function well inside cells [9]. For brain diseases, hairpin-like nanowires can be used to study neuron networks and signals without damaging the cells [10]. An analytical model for flow-guided nanonetworks has been proposed for nanonode movement in blood [11]. In health systems, nanosensors monitor the concentration level of molecules in the blood and detect infectious intra-body agents. Other healthcare systems include vital signs monitoring, detection of cardiovascular abnormalities. Drug Delivery Systems use nanoactuators to deliver nanoparticles and drugs into the body [12]. Some challenges of in-body nanocommunications are the safety

and reliability of implementing the nanodevices [13] and the effects of the THz signals on the human body [14].

In Software-Defined Metamaterials (SDMs), nanonetworks and metamaterials (artificial structures with unnatural properties) are combined, allowing the user to send commands to nanodevices aiming to perform geometrically-altering actions on the metamaterial and tuning of its electromagnetic behavior [15]. In a wider perspective of wireless communications, SDMs define a novel concept of programmable wireless environments, capable of mitigating the wireless channel losses [16].

The IoNT benefits the military and the nuclear, biological and chemical defense fields. Military nanotechnology opens the door for nanoweapons that include nano-enhanced lasers and self-replicating smart nanorobots [17]. In general, miniaturized devices such as nanosensors, nanoactuators, nanodrones and nanorobotics are implemented in smart and energy efficient battlefield monitoring systems for example [18].

To increase the productions and improve their quality, smart and sustainable agriculture systems are developed. Nanonetworks provide quick and reliable surveillance for the health of leaves and detection of any pesticides in leaves [19]. Nanonetworks for plant monitoring alert the need for water, fertilizers and pesticides. They may also intervene in animal health monitoring and feed management, where wearable sensors can be installed on cows for example [20]. Distributed air pollution control can use nanofilters [21].

2.2. Existing routing schemes in wireless networks

2.2.1. Routing schemes in wireless ad hoc networks

The traditional routing protocols (such as flooding or broadcasting schemes, Ad hoc On Demand Distance Vector (AODV) [22], Dynamic Source Routing (DSR) [23], Hierarchical routing, Optimized Link State Routing Protocol (OLSR) [24] and Greedy forwarding schemes) have limitations, either in their scalability (when networks are ultra-dense) or in their applicability (when nodes are very simple). Scalability is a problem especially for protocols that need an extended knowledge of their neighborhood (especially if they require knowledge beyond 1 hop) or that need a lot of messages and memory to maintain a correct view of their environment. Applicability mainly includes assumptions on the available hardware and resources; for instance, global positioning system (GPS), which is a given in vehicular ad hoc networks (VANET), is not feasible in potentially resource-constraint networks such as nanonetworks. Received signal strength indicator (RSSI), which is often used

as an alternative distance measuring technique, may not be available either in very simple transceivers. Memory and computational power may also be heavily restricted.

2.2.2. Routing schemes in electromagnetic nanonetworks

Some simple routing schemes which are appropriate to nanonetworks are: pure flooding, probabilistic flooding, backoff flooding and Stateless Linear-path Routing (SLR), explained in the following. In *pure flooding*, every node in the network forwards the data packet that it receives for the first time. This flooding is not scalable and results in redundant transmissions and broadcast storms in dense environments.

In *probabilistic flooding* [25], nodes forward packets with a static probability and discard it otherwise. The probability should be carefully chosen depending on the scenario, in order to guarantee the message delivery with a minimal number of forwarders.

Backoff flooding [26] is a highly efficient flooding scheme, where the number of forwarders is notably reduced. Only nodes receiving few copies of data packets (less than redundancy r) forward the packet. The count of data copies is done in a time window proportional to the number of neighbors, estimated using the node density estimator DEDeN [27]. DEDeN (Density Estimator for Dense Networks [27]) finds the node density of nodes in ultra-dense networks and nanonetworks, as follows. In DEDeN, nodes distributively estimate the local density without having to rely on a full (and very costly) exchange of hello packets. Instead, over the course of multiple rounds, they have an increasing probability to replay to a small probe packet. At each round, they also count the number of probes received. Knowing the sending probability, nodes can compute with an increasing confidence their number of neighbors.

SLR [28] is a zone-cast routing scheme that creates an anchor-based coordinate system for nanonodes that can extend to a 3D environment. Node coordinates are represented as hop counts from the anchors. Thus, space is divided in zones, where all nodes in a zone share the same coordinates. Contrarily to IP networks where the forwarding router is chosen by the preceding router, a nanonode takes the forwarding decision for itself. Only nodes whose coordinates fulfill the line equation joining the source-destination pair are forwarders. Therefore, SLR limits the zone of forwarding to the path between the source and the destination and thus also reduces the number of forwarders in the network. On the other hand, all the nodes in the zone be-

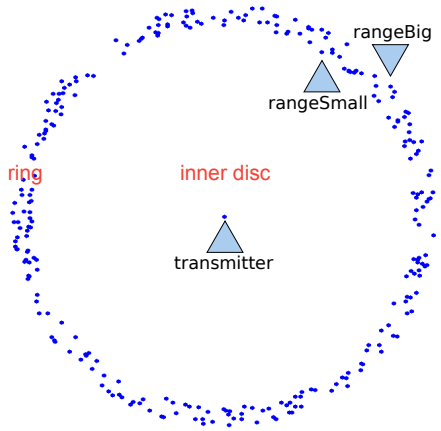

Figure 2: Ring principle: only nodes in the ring (between rangeBig and rangeSmall) are potential forwarders of the packet sent by the central node.

tween the source and the destination are forwarders and there are still some redundant retransmissions that can be eliminated.

2.2.3. Original ring

The original ring method [5], shown in Fig. 2, aims to reduce the number of forwarders. It is useful in routing in dense networks where at each hop numerous nodes are potential forwarders, and making all of them forward is inefficient, energy consuming and can create collisions and network congestion. As an example, the number of forwarders is reduced by 83% (from 909 to 155) in SLR, a non optimized protocol, and by 30% (from 103 to 73) in backoff flooding, a ultra highly optimized routing protocol [5]. The ring method does not have the aforementioned constraints on scalability and applicability, and its only assumption is that nodes can send packets with different transmission powers.

It basically works like this: each node, prior to sending its *first data packet*, sends two control packets at different powers; afterwards all the transmissions occur normally. The high-power packet uses a *rangeBig* which is equal to the communication range, aiming to make the forwarding progress faster. The small-power packet uses a *rangeSmall* smaller than *rangeBig*; it is a constant value and needs to be chosen carefully for the method to be efficient.

Nodes near the sender receive both control packets, whereas nodes having

received only the high-power control packets lie on a ring near the border of the communication range. Forwarders are *only the nodes in the ring which are selected by the routing protocol to forward*. Consequently, the ring *selects* geographically the nodes acting as forwarders.

It is worthwhile to note that in a network with static nodes (which do not move), the two control packets are sent at most once per node, hence the packet overhead induced by the method is limited. In a network with mobile nodes, the control packets could be sent several times, e.g., each time the network changes, or at regular predefined intervals based on the speed of the nodes. In the extreme case where nodes move very fast, nodes can send the two control packets each time they need to send a data packet; it could be more efficient to send the two short control packets before each data packet and make forward only a fraction of neighbors, instead of sending only the data packets and make all the neighbors forward all the packets. However, given that node mobility needs a thorough investigation, in this article *we consider only static networks*.

2.2.4. 2D dynamic ring

In the dynamic ring [7], the ring of each node is initially set like in the original ring (see previous section), i.e., using the two control packets at the first data packet it sends. However, contrary to the original ring, *rangeSmall* is chosen automatically, computed as shown below, and can change whenever needed. Its value is chosen so that the ring contain N nodes among the L neighbors, as given by a density estimator such as DEDeN [27] (introduced in Section 2.2.2).

To compute the *rangeSmall* value, the ratio of ring neighbors N to the neighbors L (= local density above) should be equal (provided that nodes are uniformly placed in the network) to the ratio of the ring to the communication circle:

$$\frac{N}{L} = \frac{ringArea}{circleArea} \tag{1}$$

$$\frac{N}{L} = \frac{\pi rangeBig^2 - \pi rangeSmall^2}{\pi rangeBig^2} \tag{2}$$

In the particular case $L < N$, the *rangeSmall* value is set to zero and all neighbors become ring neighbors. Hence,

$$rangeSmall = \begin{cases} rangeBig\sqrt{1 - N/L}, & \text{if } L > N \\ 0, & \text{otherwise} \end{cases} \tag{3}$$

It is worthwhile to note that the N neighbors include not only forwarders, but also non-forwarders; non-forwarders are not only nodes that previously forwarded a copy of the data packet, but also nodes that are not chosen by the routing scheme to forward.

The ring width is dynamic because it can be changed whenever nodes need to. For this to work, control packets have sequence numbers. Nodes are on the ring of a transmitter if the high-power control packet of the highest sequence number corresponding to the transmitter is larger than the low-power control packet of the same sequence number.

In this article we extend the dynamic ring to 3D networks, and analyze its performance, especially its memory footprint, in multi-flow 3D scenarios.

2.3. Programming and simulation environment

Several simulators of electromagnetic nanonetworks have been proposed that we present in the following.

2.3.1. Nano-Sim

NS-3[1] is a widely used network simulator due to its versatility and its compatibility with a large number of network technologies. Nano-Sim [29] is the first ns-3 module for electromagnetic nanonetworks that implements the modulation scheme TS-OOK. It is the most used nanonetwork simulator because of its simple protocol stack. However, it has some deficiencies: Nano-Sim is not being upgraded and does not have enough documentation to be included in ns-3 App Store. Nano-Sim does not consider the propagation delay and does not provide energy models. It is heavy and in practice can simulate networks of up to around one thousand nodes. It does not support the visualization modules of ns-3. In this article, both the scalability and visualization are crucial features, and consequently, Nano-Sim is not the selected simulator for this study.

2.3.2. TeraSim

TeraSim [30] is another ns-3 module that overcomes some limitations of Nano-Sim. It can include both nanoscale and macroscale networks. TeraSim has documentation and is included in ns-3 App Store. TeraSim also considers the propagation delay, the path loss, the molecular absorption and the

[1] https://www.nsnam.org

spreading loss, it also implements energy models and advanced protocols for the different layers. Like Nano-Sim above, TeraSim does not support more than one thousand nodes, as its advanced protocol stack imposes huge cost on the CPU, and thus TeraSim is not convenient for large-scale networks. Nodes also cannot be visualized by the advanced ns-3 modules. Therefore, we do not select TeraSim either.

2.3.3. Vouivre

Vouivre [31] is a C++ simulator library for nanonetworks in Dynamic Physical Rendering Simulator (DPRSim). Vouivre solves the scalability issue by removing the heavy DPRSim features, and thus can simulate tens of thousands of nodes in the nanonetwork. On the contrary, Vouivre development has stopped; it uses a statistical approach and does not study the effect of the packet payload and bits. Vouivre does not support visualization either. Hence, Vouivre is not the optimal choice of our work.

2.3.4. Physical simulators

Physical simulators such as COMSOL Multiphysics[2] present a very detailed physical model, which gives accurate results, but is very costly and can simulate only very few nodes, which is irrelevant in our case.

2.3.5. BitSimulator

BitSimulator [32] is a fast C++ electromagnetic nanonetwork simulator that can simulate hundreds of thousands of nodes, with a node density of hundreds of nodes, on a classical computer. Its scalability is confirmed in the study comparing these nanonetwork simulators [33]. It also targets both routing and transport layers and is accompanied by a visualization tool called VisualTracer. It is free software and has been used to validate results of several articles[3].

In BitSimulator, nodes have nanotransceivers with configurable range. The TS-OOK model is the only available modulation scheme, with 100 fs pulses and a configurable beta per frame. Routing protocols, such as flooding or SLR, are provided, and new routing agents can be added.

Compared to the other simulators, BitSimulator is less known and mainly has these limitations: it only simulates nanonetworks and does not implement

[2] https://www.comsol.com

[3] Available at http://eugen.dedu.free.fr/bitsimulator

the link layer, nor an energy model.

However, BitSimulator is appropriate for this article as it provides fast execution, accuracy and scalability. We used it in the simulations below.

3. System model

3.1. Nanodevice's hardware architecture

An integrated nanodevice or a nanonode includes nanocomponents. It has not been built yet, due to the size restrictions imposed by the nanoscale, but active research is being done to build each of its components. A promising material for nanocomponents is graphene that is a monolayer of carbon atoms packed into a two-dimensional honeycomb lattice [34]. Usual nanocomponents are: nanosensors, a nanoantenna, a nano-electromagnetic transceiver, a nanoactuator, a nanoprocessor, a nanomemory, and a nanopower unit. Multimedia nanodevices can also have a nanocamera and a nanomicrophone. In the following, some examples are given on each component that may not have reached the nano scale, but are taking the steps towards miniaturization.

3.1.1. Nanosensors

Nanosensors are a new generation of sensors, as a nanosensor is not only a tiny sensor, but it also uses the properties of nanomaterials to perform high resolution sensing events/phenomenons. Nanosensors can be chemical (monitoring the concentration levels or the chemical and molecular compositions), biological (sensing the biomolecular interactions of cells, antibodies and DNA), or physical (measuring physical properties such as force, pressure or displacement). Nanosensors have recently been developed for detecting pesticides on fruits in a few minutes [35].

3.1.2. Nanoantennas

Nanoantennas are responsible for transmitting and receiving signals. They are much smaller than traditional antennas and thus radiate at high frequencies. Graphene is proposed for nanoantennas to radiate in the terahertz (THz) band, as the resonant frequency of graphene-based nanoantennas can be up to two orders of magnitude below that of non-carbon nanoantannas [36]. A titanium carbide nanoantenna has been manufactured using an interesting technique, as the nanoantenna can be "sprayed" directly into any object to become a smart IoNT device [37].

3.1.3. Nano-power units

Nano-power units constitute an important part of the IoNT architecture, as they provide energy to the nanosensor devices. The goal is to maximize the potential of a nanobattery and to extend its lifetime. Nanobatteries are small batteries that need to be recharged periodically. The current battery technology relies mainly on Lithium-ion batteries, but nanobatteries, constituted of nanomaterials such as carbon nanotubes and graphene [38] for their anode and cathode parts, can have greater power density and lower recharging times [39]. To tackle the issue of the limited power supply of a nanobattery, energy harvesting presents a good platform to collect mechanical (e.g., movements), vibrational (e.g., acoustic signals) or hydraulic energy (e.g., blood flows) from the environment and converting it into electrical energy [40]. It is important to define the source of energy, as its availability depends on the application. For example, Wireless Power Transfer is an external entity that vibrates to give the nanogenerator a constant energy harvesting rate [41]. Additionally, the size of the capacitor for harvested energy storage is smaller in nanosensors compared with the traditional sensors. Therefore, the energy harvesting systems in Wireless Sensor Networks (WSNs) may not always be suitable for Wireless Nano Sensor Networks (WNSNs) [42].

3.2. Modulation scheme in electromagnetic nanonetworks

Electromagnetic nanonetworks were introduced in 2010 [40]. They are networks of integrated nanosensor devices that enable a new networking paradigm that is the Internet of Nano Things [43]. The THz band (0.1–10 THz) is the selected band for nanonetworks, as it is appropriate for the small antenna sizes of nanodevices [44].

The Time Spread On-Off Keying TS-OOK [45] is a lightweight modulation for electromagnetic nanonetworks, as it is convenient for nanomachines to use extremely short electromagnetic pulses. It is important to understand that TS-OOK *does not use a signal carrier, but electromagnetic pulses.* Pulses do not use a given frequency, but a very small energy on the whole terahertz band. These pulses can be generated by their tiny antennas, and can be detected and processed with limited computation power. The bit 1 is sent as a pulse of energy, and bit 0 is defined as silence without energy consumption. The ratio between the inter-bit duration T_s and the duration of one bit T_p is known as time spreading ratio (β). β parameter can be tuned to allow applications enough time to harvest energy. β also allows the synchronization between sender and receiver. The values proposed in the

literature are $T_p = 100\,\text{fs}$ [45] and $\beta = 1000$ (cf. "The ratio between the time between pulses and the pulse duration is kept constant" [45])). The available bandwidth is very high, of the order of Tb/s, but a node is too limited to use all of it. Nanonodes have limited power, hence the communication range is very small, at the order of millimeter.

4. Extension of the dynamic ring scheme to 3D

In the dynamic 3D ring, we transform the equation 2 into 3D. The ratio of ring neighbors N to the neighbors L should be equal to the ratio of *volumes* that is the ratio of the 3D ring to the communication sphere. Hence,

$$\frac{N}{L} = \frac{ringVolume}{sphereVolume} \tag{4}$$

$$\frac{N}{L} = \frac{\frac{4\pi}{3}rangeBig^3 - \frac{4\pi}{3}rangeSmall^3}{\frac{4\pi}{3}rangeBig^3} \tag{5}$$

$$rangeSmall = \begin{cases} rangeBig\sqrt[3]{1 - N/L}, & \text{if } L > N \\ 0, & \text{otherwise} \end{cases} \tag{6}$$

4.1. The memory cost of the ring

We recall that in the dynamic ring algorithm, a node memorizes the transmitter id and the corresponding highest control packet sequence numbers, which indicate whether the node is on the ring of this forwarder or not, which allows the node to decide whether it is a potential forwarder (i.e., in the ring) or not. Nodes are on the ring of a transmitter if its high-power control packet sequence number is larger than that of its low-power control [7]. Thus, a node needs to store two sequence numbers for each of its transmitters.

Next, we compute the number of transmitters of a node. A node can receive packets from at most L nodes, where L is the number of its neighbors. Hence, the number of transmitters to memorize is at most L, and can be less if not all of its neighbors transmit packets.

Thus, the maximum memory cost of our ring method is $2sL$, where s is the size of a sequence number (2 bytes for example) and L the node density.

This cost can be further reduced by noting that it is useless to store transmitters the node is not in the ring of. We recall that the main principle of the dynamic ring is that nodes adapt their ring width to have N nodes

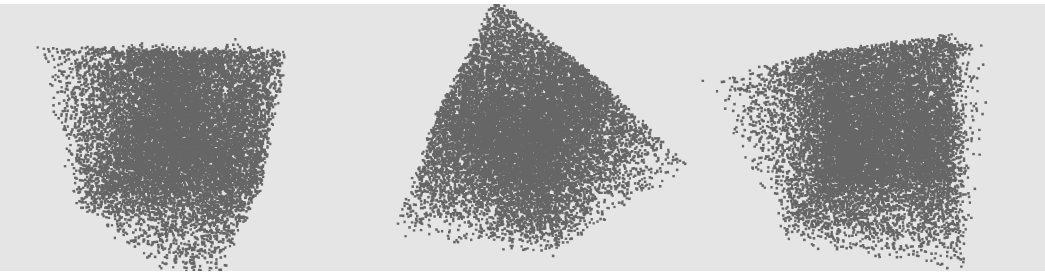

Figure 3: The 3D scenario: 15 000 nodes in a cubic space.

Table 1: Simulation parameters.

Parameter	Value
Size of simulated area	6 mm * 6 mm * 6 mm
Number of nodes	15 000
Communication range	1 000 µm
RangeBig	1 000 µm
RangeSmall	variable
Data packet size	1 003 bit
Control packet sizes	101, 102 bit

on the ring [7]. Reciprocally, a node is on the ring of approximately at most N forwarders.

Thus, the maximum memory cost of our ring method is $2sN$, with s the size of a sequence number (e.g., 2 bytes), and $N \leq L$ is the number of nodes desired in the ring.

5. Evaluation of the dynamic 3D ring scheme

5.1. Scenarios

The simulation parameters are shown in Table 1. The scenario is a nanonetwork of 15 000 nodes distributed with a homogeneous density, in three-dimensional cube space of 216 mm^3. This highly dense scenario corresponds to applications in software-defined metamaterials and in in-body communication, for example [4].

Fig. 3 shows the 3D scenario of 15 000 nodes in a cubic space.

Nodes have omnidirectional nanoantennas with a default communication range $CR = 1000$ µm and can change the range using a different transmission

power (for control packets). The network dimensions along with the communication range result in $x/CR = 6\,\text{mm} \;/\; 1\,\text{mm} = 6$ hops in each dimension, which are enough for the routing protocol evaluations. The computed average number of neighbours per node is 239.

For more realistic results, the propagation model used is the *shadowing*, with a 100% packet reception rate at distance $[0, d]$ from the transmitting node, a decreasing packet reception rate from 100% to 0% in the interval $[d, CR]$, and a zero packet reception rate at distance bigger than CR, where d is configurable. In this simulation, $d = 820\,\mu\text{m}$.

Ten random source nodes generate CBR (Constant Bit Rate) flows of 10 data packets each[4]. The flows start at the same time. A source either floods the whole network, or transmits to one random destination node[5], depending on the tested routing protocol, as shown below. Since a node sends controls only once before the very first forwarded data packet, the cost of the control packets should fade out over 10 data packets.

The packet payloads are random sequences of bits 1 and 0. The data packet size is 1003 bits and the two control packets sizes are 101 and 102 bits; these values are distinctive so that they can be spotted easily in the output log files.

Resource constraints in a nanodevice are implemented in BitSimulator through an integer parameter, called MCR (Maximum Concurrent Receptions), which represents the maximum number of concurrent receptions nodes can track in parallel (cf. "The receiver can simultaneously track a fixed number of incoming packets, K" [46]). Packets received while the node is already tracking MCR packets are discarded and ignored. In our simulations, MCR is set to 10.

The dynamic 3D ring proposed algorithm is implemented in three flooding schemes: pure flooding, probabilistic flooding and backoff flooding, and one destination-oriented scheme: SLR, all described in Section 2. For backoff flooding, the maximum number of data copies received in a time window must not exceed 2 packets in order for the node to forward ($redundancy = 2$). For

[4]The ten random source nodes have coordinates, in nm: (126 145, 2 105 389, 5 468 149), (2 824 513, 446 550, 3 419 083), (3 811 387, 536 719, 3 337 073), etc. All of them are smaller than 6 mm, the side of the world.

[5]The ten destination nodes, corresponding each to a source node, have coordinates, in nm: (1 461 843, 4 269 598, 355 469), (2 952 387, 4 013 348, 2 293 672), (1 471 109, 4 319 480, 1 317 484), etc.

probabilistic flooding, the probability value is set to the minimum probability that gives 100% delivery in each scenario, that is 60% for without the ring and 80% with dynamic ring (found empirically).

rangeBig is set to the default communication range (to increase the forwarding progress), and *rangeSmall* is dynamically chosen by nodes depending on the local density, according to Eq. 5.

The dynamic ring scheme starts with the DEDeN initialization phase in order for nodes to know their local density and compute their *rangeSmall* values. DEDeN initialization can be repeated when the network changes its topology. SLR-based routing starts with the SLR initialization phase, and the three SLR anchors are placed at the corners of the network, for nodes to locate themselves as hop counts from these anchors. CBR flows start after the DEDeN and SLR initialization phases, to not interfere with them.

To desynchronize node forwarding in ultra-dense networks and to reduce collisions, nodes choose a random backoff before forwarding, from a fixed window in pure flooding, probabilistic flooding and SLR, and from a dynamic window in backoff flooding. To avoid forwarding loops, nodes forward packets they receive for the first time only (by temporarily recording the source id and the data packet sequence numbers).

The evaluation uses the 4 routing protocols above with 2 variants each (without the ring and with dynamic 3D ring). This results in 8 simulations, where each simulation has 10 randomly generated flows of 10 data packets each.

Our 3D dynamic ring scheme aims to reduce the number of forwarders, while maintaining a 100% packet delivery ratio (PDR) to all the nodes (in flooding schemes) or the destination node (in unicast schemes). Thus, the evaluation metrics are the *number of forwarders* and the *PDR*. A good network performance means a successful packet delivery to the destination with minimum resources (forwarders). The cumulative number of forwarders per packet per flow along with the cumulative number of receivers per packet are averaged over the 10 flows and the 10 packets. The third criterion used in the evaluation is the *memory cost* of the ring, and the maximum cumulative cost that a node has ever reached is shown for each routing scheme.

5.2. Dynamic 3D ring

We recall that the ring is set at the start (at the first data packet), and *rangeSmall* is later automatically adapted so that ring has N nodes per

Table 2: Evaluation results in a 15 000 node network averaged for 10 flows with 10 packets each.

	Without ring	With dyn. 3D ring
Pure flooding:		
forwarders per packet	15 000 (100%)	2 771.4 (18.4%)
receivers per packet	15 000 (100%)	14 970 (99.8%)
Probabilistic flooding:	$p = 60\%$	$p = 80\%$
forwarders per packet	8 997 (59.9%)	2 474.2 (16.4%)
receivers per packet	14 989 (99.9%)	14 974 (99.8%)
Backoff flooding:		
forwarders per packet	562.2 (3.7%)	375.9 (2.5%)
receivers per packet	15 000 (100%)	14 999.1 (99.99%)
SLR:		
forwarders per packet	1 026.9 (6.8%)	446.9 (2.9%)
destination reached	100%	100%

hop. In the particular case where the local density is smaller than N, the *rangeSmall* value is set to zero and all neighbours become ring neighbours.

For the following simulations, we recall that the average number of neighbors per node among 15 000 nodes is 239. Among these neighbors, we use $N = 110$ for all the flooding protocols and $N = 150$ for SLR. These values are found empirically to guarantee delivery with the minimal number of forwarders. SLR needs a bigger ring than flooding protocols because SLR propagates in one direction (hence fewer potential forwarders) instead of all directions as in flooding. N value includes non-forwarders and forwarders; non-forwarders are not only nodes that previously forwarded a copy of the data packet, but also nodes that are not chosen by the routing scheme to forward.

Table 2 shows the final comparison of the average cumulative values of the 10 flows with 10 packets each for all the different combinations of the routing schemes. We provide a separate web site[6] to reproduce the results.

Effect of the dynamic ring on pure flooding. Table 2 confirms the expectations: the number of forwarders per packet is reduced by approximately 81% (from 15 000 to 2 771.4), with almost 100% delivery rate. Fig. 4 shows the

[6] http://eugen.dedu.free.fr/bitsimulator/nanocomnet23

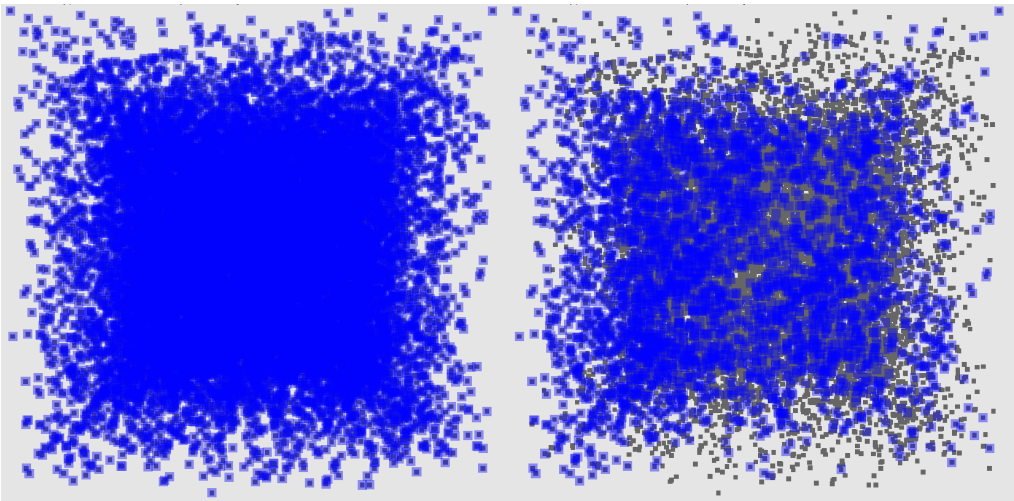

Figure 4: Pure flooding without (left) and with the dynamic 3D ring (right); forwarders in blue, first packet of the first flow only.

forwarding nodes in the network in both cases, with fewer forwarders in ring case.

The maximum cumulative cost of the ring that a certain node has ever reached is 51 transmitters in its memory, which is less than $N = 110$ ring neighbors confirming the theoretical analysis of the memory cost in 4.1. Fig. 5 displays a part of the list of nodes and the respective maximum memory cost that they have attained during routing.

Effect of the dynamic ring on probabilistic flooding. Table 2 shows that the probabilistic dynamic ring is efficient in reducing the number of forwarders per packet by approximately 72% (from 8 997 to 2 474.2), with almost 100% delivery rate. Fig. 6 shows the reduction in the number of forwarders in probabilistic flooding.

The maximum number of transmitters that a node has ever memorized is 55 transmitters, which is also less than $N = 110$ ring neighbors.

Effect of the dynamic ring on backoff flooding. The dynamic ring improves backoff flooding as seen in Table 2, where the number of relay nodes per packet decreases by approximately 33% (from 562.2 to 375.9), with almost all nodes receiving the packet ($> 99\%$). Fig. 7 shows fewer forwarders with the dynamic ring (right) compared to no ring (left). This is an exceptional result, given that backoff flooding is already a highly efficient flooding.

```
8775 onring of 22 transmitters
8831 onring of 33 transmitters
3348 onring of 27 transmitters
10113 onring of 29 transmitters
9454 onring of 17 transmitters
3969 onring of 16 transmitters
1140 onring of 27 transmitters
9539 onring of 33 transmitters
4035 onring of 23 transmitters
2938 onring of 25 transmitters
9491 onring of 11 transmitters
9216 onring of 23 transmitters
8930 onring of 28 transmitters
777 onring of 25 transmitters
900 onring of 24 transmitters
9571 onring of 20 transmitters
9563 onring of 28 transmitters
7461 onring of 26 transmitters
1208 onring of 27 transmitters
7920 onring of 26 transmitters
8801 onring of 25 transmitters
```

Figure 5: The cost of the dynamic ring in pure flooding: the first column shows the node id and the last column shows the maximum number of transmitters from which it received packets.

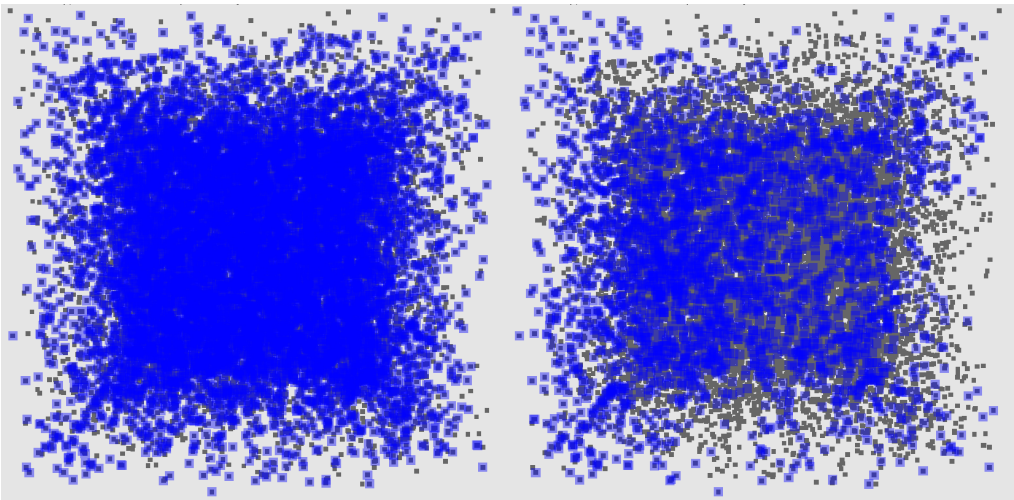

Figure 6: Probabilistic flooding without (left) and with the dynamic 3D ring (right); forwarders in blue, first packet of the first flow only.

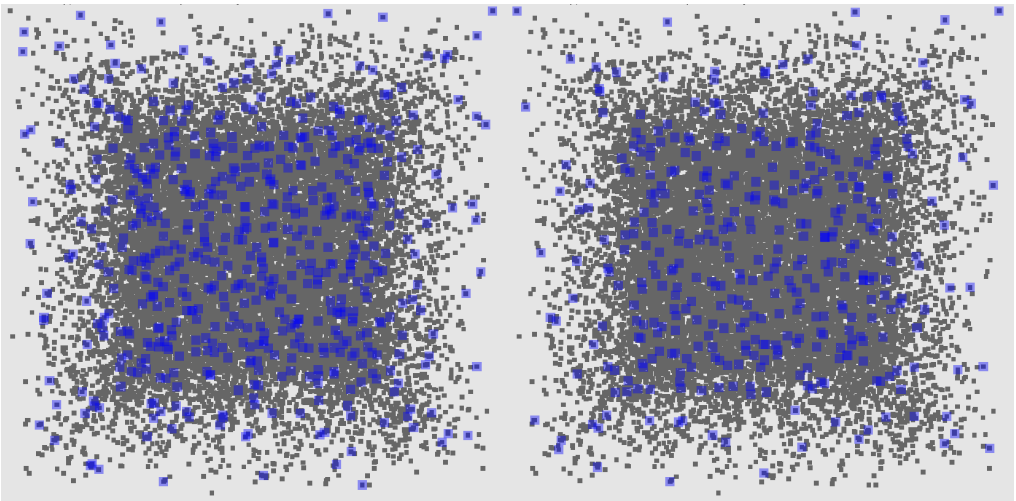

Figure 7: Backoff flooding without (left) and with the dynamic 3D ring (right); forwarders in blue, first packet of the first flow only.

The maximum cost of the ring is 132 transmitters for a node. This value is significantly larger than the previously seen routing protocols and larger than $N = 110$ ring neighbors. This is caused by the randomization of forwarder selection done by backoff flooding (i.e., random forwarders are selected each time, which increases the number of transmitters per node).

Effect of the dynamic ring on SLR. Table 2 shows that the number of forwarders is reduced by approximately 56% (from 1 026.9 to 446.9), while keeping 100% successful packet delivery. Fig. 8 visually shows this reduction of forwarders as they are on border of ranges.

The maximum cost of the ring is 81 transmitters for a node, that is less than $N = 150$ ring neighbors.

To conclude, the dynamic 3D ring optimizes all the presented routing protocols by adapting the ring width value to the 3D density. The dynamic ring selects forwarders on border of communication ranges in rings and significantly reduces the number of forwarders per packet while keeping (almost) 100% delivery rate to the destination(s).

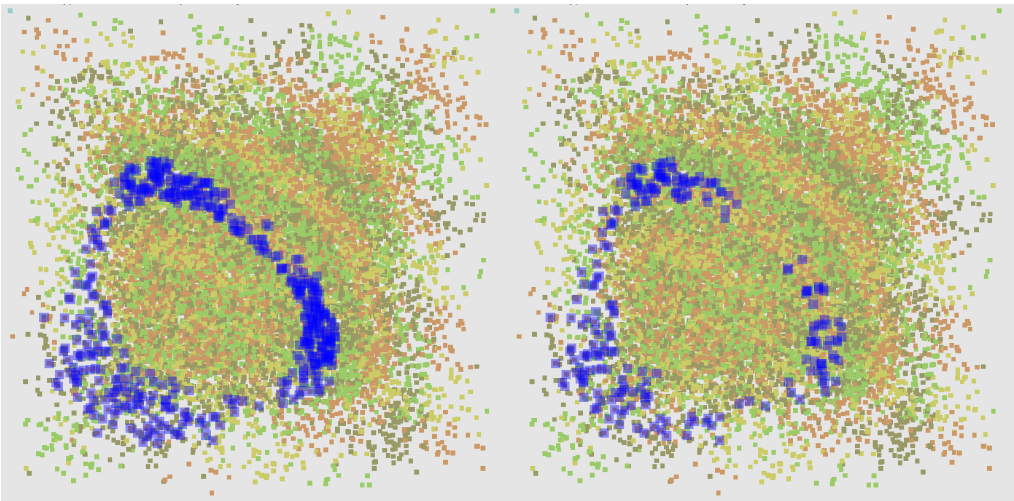

Figure 8: SLR without (left) and with the dynamic 3D ring (right); forwarders in blue, first packet of the first flow only.

6. Conclusion and future work

The ring is confirmed to work efficiently in a three-dimensional space, in a multi-source (and multi-destination) scenario. The memory cost of the ring is also evaluated and assumed to be tolerable for nanodevices. The dynamic 3D ring proves its adaptability to local densities in the space and shows a notable reduction in the number of forwarders and thus a great reduction of the required resources for routing, while maintaining good packet delivery.

Future work should concentrate on finding the optimal number and distribution of forwarders in the network, so that the resources are not wasted on redundant retransmissions. In a nanonetwork, NP-hard problems (to find the optimal number of forwarders) are too complex to solve, but we hope to still find solutions to reduce the number of forwarders. Another challenge is addressing mobility of nanodevices, as this is a characteristic of some applications.

Acknowledgments

This work has been funded by Pays de Montbéliard Agglomération (France).

References

[1] K. L. Lueth, M. Hasan, S. Sinha, S. Annaswamy, P. Wegner, F. Bruegge, M. Kulezak, A comprehensive 114-page report on the current state of the Internet of Things, incl. market update & forecast, latest trends, IT spending update, and more, Tech. rep., IoT Analytics (May 2022).

[2] I. F. Akyildiz, J. M. Jornet, M. Pierobon, Nanonetworks: A new frontier in communications, Communications of the ACM 54 (11) (2011) 84–89.

[3] N. Rikhtegar, M. Keshtgary, A brief survey on molecular and electromagnetic communications in nano-networks, International Journal of Computer Applications 79 (3) (2013).

[4] F. Lemic, S. Abadal, W. Tavernier, P. Stroobant, D. Colle, E. Alarcón, J. Marquez-Barja, J. Famaey, Survey on terahertz nanocommunication and networking: A top-down perspective, IEEE Journal on Selected Areas in Communications 39 (6) (2021) 1506–1543.

[5] F. Hoteit, E. Dedu, W. K. Seah, D. Dhoutaut, Ring-based forwarder selection to improve packet delivery in ultra-dense networks, in: IEEE Wireless Communications and Networking Conference (WCNC), IEEE, Austin, TX, USA, 2022, pp. 2709–2714.

[6] F. Hoteit, D. Dhoutaut, W. K. Seah, E. Dedu, Expanded ring-based forwarder selection to improve packet delivery in ultra-dense nanonetworks, in: International Wireless Communications and Mobile Computing Conference (IWCMC), IEEE, Dubrovnik, Croatia, 2022, pp. 1406–1410.

[7] F. Hoteit, D. Dhoutaut, W. K. Seah, E. Dedu, Dynamic ring-based forwarder selection to improve packet delivery in ultra-dense nanonetworks, in: 9th ACM International Conference on Nanoscale Computing and Communication (ACM NanoCom), ACM, Barcelona, Catalunya, Spain, 2022, p. 7.

[8] N. A. Ali, M. Abu-Elkheir, Internet of nano-things healthcare applications: Requirements, opportunities, and challenges, in: 11th Int. Conf. on Wireless and Mobile Computing, Networking and Communications (WiMob), IEEE, Los Alamitos, CA, USA, 2015, pp. 9–14.

[9] J. T. Devreese, Importance of nanosensors: Feynman's vision and the birth of nanotechnology, MRS bulletin 32 (9) (2007) 718–725.

[10] X. Zhang, Nanowires pin neurons: a nano "moon landing", Matter 1 (3) (2019) 560–562.

[11] S. Canovas-Carrasco, R. Asorey-Cacheda, A.-J. Garcia-Sanchez, J. Garcia-Haro, K. Wojcik, P. Kulakowski, Understanding the applicability of terahertz flow-guided nano-networks for medical applications, IEEE Access 8 (2020) 214224–214239.

[12] R. Iovine, V. Loscrì, S. Pizzi, R. Tarparelli, A. M. Vegni, Electromagnetic nanonetworks for sensing and drug delivery, in: Modeling, Methodologies and Tools for Molecular and Nano-scale Communications, Springer, 2017, pp. 473–501.

[13] F. Dressler, S. Fischer, Connecting in-body nano communication with body area networks: Challenges and opportunities of the internet of nano things, Nano Communication Networks 6 (2) (2015) 29–38.

[14] N. Saeed, M. H. Loukil, H. Sarieddeen, T. Y. Al-Naffouri, M.-S. Alouini, Body-centric terahertz networks: Prospects and challenges, IEEE Transactions on Molecular, Biological and Multi-Scale Communications (2021).

[15] C. Liaskos, A. Tsioliaridou, A. Pitsillides, I. F. Akyildiz, N. V. Kantartzis, A. X. Lalas, X. Dimitropoulos, S. Ioannidis, M. Kafesaki, C. Soukoulis, Design and development of software defined metamaterials for nanonetworks, IEEE Circuits and Systems Magazine 15 (4) (2015) 12–25.

[16] C. Liaskos, S. Nie, A. Tsioliaridou, A. Pitsillides, S. Ioannidis, I. Akyildiz, A new wireless communication paradigm through software-controlled metasurfaces, IEEE Communications Magazine 56 (9) (2018) 162–169.

[17] L. A. Del Monte, Nanoweapons: A Growing Threat to Humanity, U of Nebraska Press, 2017.

[18] P. Fraga-Lamas, T. M. Fernández-Caramés, M. Suárez-Albela, L. Castedo, M. González-López, A review on internet of things for defense and public safety, Sensors 16 (10) (2016) 1644.

[19] A. Zahid, H. T. Abbas, A. Ren, A. Alomainy, M. A. Imran, Q. H. Abbasi, Application of terahertz sensing at nano-scale for precision agriculture, Wireless Automation as an Enabler for the next Industrial Revolution (2020) 241–257.

[20] A. Awasthi, A. Awasthi, D. Riordan, J. Walsh, Non-invasive sensor technology for the development of a dairy cattle health monitoring system, Computers 5 (4) (2016) 23.

[21] J. Han, J. Fu, R. B. Schoch, Molecular sieving using nanofilters: past, present and future, Lab on a Chip 8 (1) (2008) 23–33.

[22] C. Perkins, E. Belding-Royer, S. Das, Ad hoc on-demand distance vector (AODV) routing, Tech. rep., IETF RFC 3561 (2003).

[23] D. Johnson, Y.-c. Hu, D. Maltz, The dynamic source routing protocol (dsr) for mobile ad hoc networks for ipv4, Tech. rep., IETF RFC 4728 (2007).

[24] T. Clausen, P. Jacquet, Optimized link state routing protocol (olsr), Tech. rep., IETF RFC 3626 (2003).

[25] D. G. Reina, S. Toral, P. Johnson, F. Barrero, A survey on probabilistic broadcast schemes for wireless ad hoc networks, Ad Hoc Networks 25 (2015) 263–292.

[26] T. Arrabal, D. Dhoutaut, E. Dedu, Efficient multi-hop broadcasting in dense nanonetworks, in: 17th IEEE International Symposium on Network Computing and Applications (NCA), IEEE, Cambridge, MA, USA, 2018, pp. 385–393.

[27] T. Arrabal, D. Dhoutaut, E. Dedu, Efficient density estimation algorithm for ultra dense wireless networks, in: International Conference on Computer Communications and Networks (ICCCN), IEEE, Hangzhou, China, 2018, pp. 1–9.

[28] A. Tsioliaridou, C. Liaskos, E. Dedu, S. Ioannidis, Packet routing in 3D nanonetworks: A lightweight, linear-path scheme, Nano Communication Networks 12 (2017) 63–71.

[29] G. Piro, L. A. Grieco, G. Boggia, P. Camarda, Nano-Sim: simulating electromagnetic-based nanonetworks in the network simulator 3, in: 6th International ICST Conference on Simulation Tools and Techniques (SimuTools), ACM, Cannes, France, 2013, pp. 203–210.

[30] Z. Hossain, Q. Xia, J. M. Jornet, TeraSim: An *ns-3* extension to simulate Terahertz-band communication networks, Nano Communication Networks 17 (2018) 36–44.

[31] N. Boillot, D. Dhoutaut, J. Bourgeois, Going for large scale with nano-wireless simulations, in: 2nd ACM International Conference on Nanoscale Computing and Communication (NanoCom), ACM, Boston, MA, USA, 2015, pp. 1–2.

[32] D. Dhoutaut, T. Arrabal, E. Dedu, BitSimulator, an electromagnetic nanonetworks simulator, in: 5th ACM/IEEE International Conference on Nanoscale Computing and Communication (NanoCom), ACM/IEEE, Reykjavik, Iceland, 2018, pp. 1–6.

[33] E. Sahin, O. Dagdeviren, M. A. Akkas, An evaluation of internet of nano-things simulators, in: 6th International Conference on Computer Science and Engineering (UBMK), IEEE, Ankara, Turkey, 2021, pp. 670–675.

[34] A. K. Geim, K. S. Novoselov, The rise of graphene, in: Nanoscience and technology: a collection of reviews from nature journals, World Scientific, 2010, pp. 11–19.

[35] H. Li, P. Merkl, J. Sommertune, T. Thersleff, G. A. Sotiriou, SERS hotspot engineering by aerosol self-assembly of plasmonic ag nanoaggregates with tunable interparticle distance, Advanced Science (2022) 2201133.

[36] J. M. Jornet, I. F. Akyildiz, Graphene-based nano-antennas for electromagnetic nanocommunications in the terahertz band, in: 4th European Conference on Antennas and Propagation, IEEE, Barcelona, Spain, 2010, pp. 1–5.

[37] A. Sarycheva, A. Polemi, Y. Liu, K. Dandekar, B. Anasori, Y. Gogotsi, 2D titanium carbide (MXene) for wireless communication, Science advances 4 (9) (2018) eaau0920.

[38] W. G. Soliman, C. Swathi, T. Yasasvi, B. K. Priya, D. A. Reddy, Review on poly (ethylene oxide)-based electrolyte and anode nanomaterials for the internet of things node-level lithium-ion batteries, Materials Today: Proceedings 42 (2021) 429–435.

[39] K. Wong, S. Dia, Nanotechnology in batteries, Journal of Energy Resources Technology 139 (1) (2017).

[40] I. F. Akyildiz, J. M. Jornet, Electromagnetic wireless nanosensor networks, Nano Communication Networks 1 (1) (2010) 3–19.

[41] M. Donohoe, S. Balasubramaniam, B. Jennings, J. M. Jornet, Powering in-body nanosensors with ultrasounds, IEEE Transactions on Nanotechnology 15 (2) (2015) 151–154.

[42] J. M. Jornet, I. F. Akyildiz, Joint energy harvesting and communication analysis for perpetual wireless nanosensor networks in the terahertz band, IEEE Transactions on Nanotechnology 11 (3) (2012) 570–580.

[43] I. F. Akyildiz, J. M. Jornet, The internet of nano-things, IEEE Wireless Communications 17 (6) (2010) 58–63.

[44] J. M. Jornet, I. F. Akyildiz, Channel capacity of electromagnetic nanonetworks in the terahertz band, in: 2010 IEEE international conference on communications, IEEE, 2010, pp. 1–6.

[45] J. M. Jornet, I. F. Akyildiz, Femtosecond-long pulse-based modulation for Terahertz band communication in nanonetworks, IEEE Transactions on Communications 62 (5) (2014) 1742–1753.

[46] J. C. Pujol, J. M. Jornet, J. S. Pareta, PHLAME: A physical layer aware MAC protocol for electromagnetic nanonetworks, in: 2011 IEEE Conference on Computer Communications Workshops (INFOCOM WKSHPS), IEEE, Shanghai, China, 2011, pp. 431–436.